Coexistence of Magnetic and Delocalized Electrons in Hybrid Molecular Materials. The Series of Organic–Inorganic Radical Salts (BEDT-TTF)$_8$[XW$_{12}$O$_{40}$](solv)$_n$ (X = 2(H$^+$), B^{III}, Si^{IV}, Cu^{II}, Co^{II}, Fe^{III}; solv = H$_2$O, CH$_3$CN)

Carlos J. Gómez-García,*[†,⊥] Carlos Giménez-Saiz,[†] Smaïl Triki,[†] Eugenio Coronado,*[†] Pierre Le Magueres,[‡] Lahcène Ouahab,*[‡] Laurent Ducasse,[§] Claude Sourisseau,[||] and Pierre Delhaes*[⊥]

Dept. Química Inorgánica, Universitat de Valencia, Dr. Moliner 50, 46100 Burjasot, Spain, LCSIM, URA 1495, CNRS, Avenue Général Leclerc, 35042 Rennes, France, LPCT, URA 503, CNRS, 351 Cours de la Libération, 33405 Talence, France, LSMC, URA 0124, Univ. de Bordeaux I, 351 Cours de la Libération, 33405 Talence, France, and CRPP, CNRS, Avenue Albert Schweitzer, 33600 Pessac, France

The synthesis, crystal structure and physical properties of the new series α_1 and α_2 of radical salts made with bis(ethylenedithio)tetrathiafulvalene (BEDT-TTF or ET) and Keggin polyoxoanions are reported. The structure of the α_1-ET$_8$[XW$_{12}$O$_{40}$] (X = Co^{II}, Cu^{II}, 2(H$^+$) and Fe^{III}) series (crystal data: α_1-ET$_8$[CoW$_{12}$O$_{40}$]·5.5H$_2$O (**I**), monoclinic, space group I2/m, a = 13.971(9) Å, b = 43.117(7) Å, c = 14.042(5) Å, β = 107.25(3)°, V = 8078 Å^3, Z = 2; α_1-ET$_8$[FeW$_{12}$O$_{40}$]·9H$_2$O (**II**), monoclinic, space group *I2/m*, a = 13.955(10) Å, b = 43.221(7) Å, c = 14.049(3) Å, β = 107.24(4)°, V = 8093 Å^3, Z = 2) consists of alternating layers of the organic donor and the Keggin polyoxometalates. The organic layers contain three crystallographically independent molecules that form two different parallel stacks alternating in the [10$\bar{1}$] direction. The structure of the α_2-ET$_8$[XW$_{12}$O$_{40}$] (X = Co^{II}, Cu^{II}, 2(H$^+$), Fe^{III} and B^{III}) series (crystal data: α_2-ET$_8$[CoW$_{12}$O$_{40}$]·0.5CH$_3$CN·3H$_2$O (**III**), monoclinic, space group *I2/m*, a = 16.66(2) Å, b = 43.42(2) Å, c = 12.14(1) Å, β = 111.78(9)°, V = 8151 Å^3, Z = 2; α_2-ET$_8$[BW$_{12}$O$_{40}$]·2H$_2$O (**IV**), monoclinic, space group *I2/m*, a = 16.50(1) Å, b = 43.27(2) Å, c = 12.125(3) Å, β = 111.99(4)°, V = 8026 Å^3, Z = 2) is similar to that of the α_1 phase but the organic layers contain only two crystallographically independent molecules. In both α phases the Keggin polyanions form closed packed pseudohexagonal layers. Both crystal structures suggest the presence of two types of differently charged stacks: a dimerized one with almost neutral ET molecules, and an eclipsed one formed by almost ionized ET molecules. This inhomogeneous charge distribution is confirmed by Raman spectroscopy. Conductivity measurements show that all compounds are semiconductors, in agreement with the band structure EHT calculations. Magnetic measurements indicate the presence of antiferromagnetic interactions in the organic sublattice with the presence of a strong Curie tail and confirm the electronic distribution in the two kinds of stacks. ESR spectra of the salts with diamagnetic anions complete these results and for the radical salts with paramagnetic anions indicate that both sublattices coexist but do not interact significantly.

Introduction

The research field based on the design and synthesis of new molecular compounds presenting interesting physical properties is supported by the concept of interacting electrons. Indeed it has been shown that for atomic solids several specific physical properties are associated with the presence of narrow electronic bands when the charge carriers are interacting both with the lattice vibrations and between them.[1] These interactions give rise to phenomena such as the metal–insulator transition of Mott–Hubbard type or the occurrence of a cooperative ordered state at low temperature, namely the competing superconducting (SC) and magnetic ground states. A more recent approach has been to extend these researches to charge transfer molecular solids which can also give rise, in chemistry language, to mixed valency systems. These are the new classes of charge transfer salts and, in particular, the radical cation salts which are issued

from the tetrathiafulvalene (TTF) derivatives and other donor molecules.[2]

These molecular associations offer several advantages; in particular, the possibility of combining a large variety of organic and inorganic blocks which allows us to create new structural organizations with electronic or magnetic properties of restricted dimensionality. The last improvements in this research domain have been the discovery of 2-d mixed valence compounds which present higher transition temperatures for either the SC or the AF transition than those of the quasi 1-d systems, the so called Bechgaard's salts.[3] Because of the rich polymorphism found in these salts of bis(ethylenedithio)tetrathiafulvalene (BEDT-TTF or ET) or analog molecules, several types of molecular organizations have been defined as for example the archetypical α, β, or κ phase salts.[4] They are always characterized by organic layers where a π delocalized system is present separated by

[†] Universitat de Valencia.
[‡] URA 1495, CNRS.
[§] URA 503, CNRS.
[||] Univ. de Bordeaux.
[⊥] CRPP, CRNS.
[⊗] Abstract published in *Advance ACS Abstracts*, July 1, 1995.
(1) Mott, N. F. *Metal-Insulator Transitions*; Taylor, Francis, Eds.; 1990.

(2) Delhaès, P. In NATO ASI *Lower-Dimensional Systems and Molecular Electronics*; Metzger, R. M., Day, P., Papavassiliou, G. C., Eds.; Plenum Press: New York, 1991; p 43.
(3) Jerome, D. *Science* **1991**, *252*, 1514.
(4) Williams, J. M.; Ferraro, J. R.; Thorn, R. J.; Carlson, K. D.; Geiser, U.; Wang, H. H.; Kini, A. M.; Whangbo, M. H. In *Organic Superconductors. Synthesis, Structure, Properties, and Theory*; Grimes, R. N., Ed.; Prentice Hall: Englewood Cliffs, NJ, 1992.

sheets of the inorganic counterions which appear to play a crucial role in the physical properties.

Following these general arguments, several combined strategies have been proposed concerning the counterions:

(i) With radical cation salts, the use of bulky polyanions[5] for which the spatial organization can be different with, in particular, an increased dimensionality, besides the possibility of variation of the anionic charge, opens the way to modulate the electronic band filling in the resulting salt and, therefore, the physical properties.

(ii) The introduction of magnetic moments thanks to transition metals in these anions, is a complementary aspect because it opens a new type of interactions between the π electrons and the localized magnetic ions,[6] the so-called indirect exchange interaction.

In this context, it appears that polyoxometalates[7] present several characteristics which make them suitable as inorganic components of new radical cation salts: (i) These molecular metal oxides can have large different charges while maintaining identical the shape and size of the anion; (ii) they are soluble in aqueous and non aqueous solutions and they maintain their identities in solution as well as in the solid state; (iii) they are electron acceptors which can be reduced by one or more electrons, giving rise to mixed valency clusters; (iv) they can act as ligands incorporating at specific sites of the polyoxoanion structure one or more transition metal ions.

Taking advantge of the two former characteristics, several examples have been reported containing diamagnetic polyoxoanions of the type $[X^{n+}M_{12}O_{40}]^{(8-n)-}$ ($X^{n+} = P^V$, Si^{IV}; M = W, Mo),[5,8] $[M_6O_{19}]^{2-}$ (M = Mo, W)[9] and $[Mo_8O_{26}]^{4-}$ anion.[10] The ability of the polyoxoanion to accept electrons from the organic donor (point iii) has also been observed in some cases, giving rise to materials in which delocalized electrons coexist in both the organic and the inorganic units.[5c] Very recently we have started to exploit point iv with the aim to introduce a magnetic character in the polyoxoanion.[11] Following this approach we have prepared[12] an extensive family of cation radical salts by using as organic donor the ET and, as inorganic

anions, diamagnetic and paramagnetic polyoxometalates with the Keggin structure[13] $[XW_{12}O_{40}]^{(8-n)-}$ ($X^{n+} = Co^{II}$, Cu^{II}, Fe^{III}, $2(H^+)$, Zn^{II}, B^{III} and Si^{IV}). These new materials present an α type of packing of the organic donors[4] in two different crystallographic phases with the general formula: ET_8-$[XW_{12}O_{40}](solv)_n$ (solv = H_2O, CH_3CN).

In this paper, after a description of the crystal preparation, we report the crystal and electronic structures of these materials in relation to their physical properties. In particular we have studied the spectroscopic properties (IR, absorption Raman scattering) which give a local information on the molecular degree of ionicity, as well as dc conductivity and magnetic properties, which are, on the contrary, bulk properties. Indeed, static but also dynamic (i.e., ESR) magnetic investigations allow us to describe the magnetic exchange processes within the organic part as well as, when the polyoxometalates are paramagnetic, between the organic and inorganic sublattices.

Experimental Section

Synthesis. All the radical salts were obtained on a platinum wire electrode by anodic oxidation of the organic donor ET (2×10^{-3} M) in an U-shaped electrocrystallization cell under low constant current ($I = 0.6$ μA) in the presence of the tetrabutyl- (TBA$^+$) or tetraethyl-ammonium (TEA$^+$) salts of the polyanions (10^{-2} M) as supporting electrolyte. These salts were prepared by metathesis of concentrated solutions of the Na$^+$ or K$^+$ salts, synthesized according to the literature procedures,[13] in acidic (HNO$_3$) medium. The so-prepared TBA$^+$ or TEA$^+$ salts were recrystallized twice in acetonitrile or in dimethylformamide prior to their use in the electrochemical cells. These recrystallization conditions yielded in all cases well formed single crystals whose purity was checked by metal analysis and IR spectroscopy. The solvents were not previously dried, and in all cases it was necessary to add some drops of water in the anodic compartment of the cell in order to obtain good quality single crystals, suggesting that either the water or the protons (or both) are necessary for the crystallization of the salts. All the crystals were collected, washed with CH$_3$CN and CH$_2$Cl$_2$ (to remove any portion of neutral ET crystals or the TBA$^+$ salts of the polyanions), and air-dried. Depending on the electrocrystallization conditions, three different crystallographic phases, denoted as α_1, α_2, and a third unidentified phase (see below), were obtained from nearly all the polyanions. Amber platelike single crystals of the α_1 phase ($X^{n+} = Co^{II}$, Cu^{II}, Fe^{III}, $2(H^+)$ and Si^{IV}) were obtained when a mixture of CH$_2$Cl$_2$ and CH$_3$CN in the 3:1 ratio was used as solvent; dark brown needle-like single crystals of the α_2 phase ($X^{n+} = Co^{II}$, Cu^{II}, Fe^{III}, $2(H^+)$ and B^{III}) were obtained with a mixture of the same solvents in a 1:1 ratio. Finally, very thin platelike shiny brown-golden crystals of the third, unidentified, phase were obtained for different solvent conditions, although a mixture of CH$_2$Cl$_2$ and ethanol in a 3:1 ratio seems to be the best one. This last phase was obtained for six different Keggin-type polyanions ($[XW_{12}O_{40}]^{(8-n)-}$, $X^{n+} = Co^{II}$, Cu^{II}, Fe^{III}, $2(H^+)$, B^{III} and Zn^{II}). The IR spectra of these salts indicated the presence of TBA$^+$ counterions and elemental analysis gave a proportion ET:TBA:$[XW_{12}O_{40}]$ of 4:3:1.[15] The stoichiometry and content of solvent

(5) (a) Ouahab, L.; Bencharif, M.; Grandjean, D. *C. R. Acad. Sci. Paris, Sér. 2* **1988**, *307*, 749. (b) Ouahab, L.; Triki, S.; Grandjean, D.; Bencharif, M.; Garrigou-Lagrange, C.; Delhaès, P. In ref 2. (c) Ouahab, L.; Bencharif, M.; Mhanni, A.; Pelloquin, D.; Halet, J. F.; Peña, O.; Padiou, J.; Grandjean, D.; Garrigou-Lagrange, C.; Amiell, J.; Delhaès, P. *Chem. Mater.* **1994**, *4*, 666. (d) Ouahab, L. In ref 7c.

(6) (a) Maceno, G. Ph.D. Dissertation. University of Bordeaux, France, 1988. (b) Lequan, M.; Lequan, R. M.; Hauw, C.; Gaultier, J.; Maceno, G.; Delhaès, P. *Synth. Met.* **1987**, *19*, 409. (c) Mallal, T.; Hollis, C.; Bott, S.; Day, P.; Kurmoo, M. *Synth. Met.* **1988**, *27*, A381. (d) Mori, T.; Wang, P.; Imaeda, K.; Enoki, T.; Inokuchi, H.; Sakai, F.; Saito, G. *Synth. Met.* **1988**, *27*, A451. (e) Day, P.; Kurmoo, M.; Mallah, T.; Marsden, I. R; Friend, R. H.; Pratt, F. L.; Hayes, W.; Chasseau, D.; Gaultier, J.; Bravic, G.; Ducasse, L. *J. Am. Chem. Soc.* **1992**, *114*, 10722. (f) Kurmoo, M.; Day, P.; Allan, M.; Friend, R. H. *Mol. Cryst. Liq. Cryst.* **1993**, *234*, 199–204.

(7) (a) Pope, M. T. *Heteropoly and Isopoly Oxometalates*, Springer-Verlag: Berlin, 1983. (b) Pope, M. T.; Müller, A. *Angew. Chem.* **1991**, *103*, 56; *Angew. Chem., Int. Ed. Eng.* **1991**, *30*, 34; (c) *Polyoxometalates: from Platonic Solids to Anti-retroviral activity*; Pope, M. T.. Müller, A., Eds. Kluwer Acad. Pub.: Dordrecht, The Netherlands, 1994.

(8) (a) Davidson, A.; Boubekeur, K.; Pénicaud, A.; Auban, P.; Lenoir, C.; Batail, P.; Hervé, G. *J. Chem. Soc., Chem. Commun.* **1989**, 1373. (b) Bellito, C.; Bonamico, M.; Staulo, G. *Mol. Cryst. Liq. Cryst.* **1993**, *232*, 155.

(9) (a) Triki, S.; Ouahab, L.; Padiou, J.; Grandjean, D. *J. Chem. Soc., Chem. Commun.* **1989**, 1608. (b) Triki, S.; Ouahab, L.; Grandjean, D.; Fabre. J. M. *Acta Crystallogr.* **1991**, *C47*, 645. (c) Triki, S.; Ouahab. L.; Halet, J. F.; Peña, O.; Padiou, J.; Grandjean, D.; Garrigou-Lagrange, C.; Delhaès, P. *J. Chem. Soc., Dalton Trans.* **1992**, 1217.

(10) Gómez-García, C. J.; Coronado, E.; Triki, S.; Ouahab, L.; Delhaès, P. *Adv. Mater.* **1993**, *4*, 283.

(11) (a) Gómez-García, C. J.; Borrás-Almenar, J. J.; Coronado, E.; Delhaès, P.; Garrigou-Lagrange, C.; Baker, L. C. W. *Synth. Met.* **1993**, *55–57*, 2023. (b) Coronado, E.; Gómez-García, C. J. In ref. 7c. (c) Coronado, E.; Gómez-García, C. J. *Comments Inorg. Chem.*, in press.

(12) Gómez-García, C. J.; Ouahab, L.; Gimenez-Saiz, C.; Triki, S.; Coronado, E.; Delhaès, P. *Angew. Chem.* **1994**, *106*, 234, *Angew. Chem., Int. Ed. Engl.* **1994**, *33*, 223.

(13) (a) Keggin, J. F. *Nature* **1933**, *131*, 908. (b) Keggin, J. F. *Proc. R. Soc. London, A* **1934**, *144*, 75.

(14) (a) Mair, J. A. *J. Chem. Soc.* **1950**, 2364. (b) Simmons, V. E. Doctoral Dissertation, Boston University, 1963; *Diss. Abstr.* **1963**, *24*, 1391. (c) Nomiya, K.; Miwa, M.; Kobayashi, R.; Aiso, M. *Bull. Chem. Soc. Jpn.* **1981**, *54*, 2983 and references therein.

(15) Unfortunately, the crystals of this third phase are twined so that no X-ray structure determination could be carried out. In any case, the powder X-ray diffraction spectra for the six mentioned salts are the same and are different from those of the α phases, confirming the existence of a third different phase.

Table 1. Unit Cell Parameters[e] for the α_1 (1−5) and α_2 (6−10) Series of the Radical Salts $ET_8[XW_{12}O_{40}]$

no	phase-X	a (Å)	b (Å)	c (Å)	β (°)	V (Å³)
1	α_1-Co^{II} [c]	13.971(9)	43.117(7)	14.042(5)	107.25(3)	8078
2	α_1-Cu^{II} [b]	13.99(4)	43.32(3)	14.027(7)	106.81(13)	8137
3	α_1-Fe^{III} [c]	13.955(10)	43.221(7)	14.049(3)	107.24(5)	8093
4	α_1-2H$^+$ [a]	14.02(2)	43.0(1)	14.12(1)	107.18(9)	8130
5	α_1-Si^{IV} [d]	14.017(3)	43.259(6)	14.065(5)	107.26(2)	8144
6	α_2-Co^{II} [c]	16.66(2)	43.42(2)	12.14(1)	111.78(9)	8151
7	α_2-Cu^{II} [b]	16.562(6)	43.41(3)	12.190(6)	111.77(4)	8139
8	α_2-Fe^{III} [b]	16.75(2)	43.27(3)	12.151(9)	111.49(6)	8192
9	α_2-2(H$^+$) [b]	16.711(7)	43.23(3)	12.15(1)	111.96(4)	8139
10	α_2-B^{III} [c]	16.50(1)	43.27(2)	12.125(3)	111.99(4)	8026

[a] Unit cell parameters determined from X-ray powder diffraction data. [b] Unit cell parameters determined from single crystal X-ray data. [c] Compounds whose structure has been fully determined by single crystal analysis. [d] From ref 8a. [e] Numbers in parentheses are estimated standard deviations in the least significant digits.

molecules (H_2O and CH_3CN) of both α phases were only determined from the X-ray structure.

X-ray Crystallography. The unit cell parameters were determined from either single crystal or X-ray powder patterns (see Table 1). The powder diffraction data were registered on a Rigaku diffractometer equipped with a Cu Kα radiation $\lambda = 1.540\,51$ Å. The powder diffraction patterns were indexed by reference to the α_1 and α_2 phases. The unit cell parameters were refined by least-squares methods using the peak positions (2θ). The X-ray crystal structures were determined for two salts with the α_1 structure: α_1-$ET_8[CoW_{12}O_{40}]\cdot 5.5H_2O$ and α_1-$ET_8[FeW_{12}O_{40}]\cdot 9H_2O$ and two salts with the α_2 structure: α_2-ET_8-$[BW_{12}O_{40}]\cdot 2H_2O$ and α_2-$ET_8[CoW_{12}O_{40}]\cdot 0.5CH_3CN\cdot 3H_2O$ (see Table 2). The crystals, which are stable in air, were mounted on an Enraf-Nonius CAD4 diffractometer equipped with a graphite crystal, incident beam monochromator. Preliminary examination and data collection were performed with Mo Kα radiation. Cell constants and an orientation matrix for data collection were obtained from least-squares refinement, using the setting angles of 25 reflections. During data collection three standard reflections were measured every hour and showed no significant decay. Lorentz, polarization and a semiempirical absorption correction (ψ-scan method)[16] were applied to the intensity data. Other important features of the crystal data are summarized in Table 2. Among the three possible monoclinic space groups,[17] $I2$, Im and $I2/m$, corresponding to the extinction conditions, the latter was retained on the basis of the successful solution and refinement of the structures. All calculations were performed on a VAX computer using MolEN.[18] The structures were solved by direct methods using MULTAN[19] and were developed with successive full-matrix least-squares refinements and difference Fourier syntheses, which showed all the atoms of organic donors, the polyanion, and the solvent molecules. On the contrary to the ET molecules, which show no evident crystallographic disorder, the Keggin anions appear as centrosymmetric units as a result of a disorder due to a rotation of 90° around the C_2 axis of the central tetrahedron. This kind of disorder has been found in other crystal structures with Keggin anions surrounded by big and weakly polarizing cations[5,20] as clearly described and explained by Pope

and Evans.[21] A direct consequence of this disorder is the impossibility of refining all the oxygen atoms of the anion with anisotropic thermal parameters. Nevertheless, the reliability factors are in the normal range found for other polyoxometalate salts.[22]

Conductivity Measurements. Temperature dependence of the dc conductivity over the range 10−300 K was measured by use of a phase detector using the standard four probe technique. Conductivity measurements were performed on several single crystals for each of the three salts that gave suitable single crystals. Contacts to the crystals were made by gold wires attached with silver paint. The configurations used were function on the size and shape of the plate-like single crystals.

Magnetic Measurements. Variable temperature susceptibility measurements were carried out in the temperature range 2−300 K at a magnetic field of 0.1 T on polycrystalline samples with a magnetometer (905 VTS, SHE Corp.) equipped with a SQUID sensor. The susceptibility data were corrected from the diamagnetic contributions of the ET molecules (-201.6×10^{-6} emu·mol^{-1} per ET molecule, as deduced by using Pascal's constant tables) and from the diamagnetic and TIP contributions of the Keggin units (these contributions were calculated from the susceptibility measurements of the TBA$^+$ salts of the corresponding Keggin anions, and are similar to those applied in other radical salts of TTF with Keggin polyanions).[5c] Variable-temperature ESR spectra of single crystals were recorded at X-band with a Varian E109 spectrometer equipped with a helium cryostat. Angular dependence of the ESR spectra was measured by the use of a homemade goniometer. The single crystals were mounted with silicon grease on quartz rods. The field was measured using a diphenylpicrylhydrazyl (DPPH, $g = 2.0036$) stable free radical marker.

Infrared, Raman, and UV−Vis Spectroscopies. IR spectra were recorded in the range 400−4700 cm^{-1} at different temperatures (300−15 K) on pressed KBr pellets with a Nicolet MX-1 FT-IR interferometer and on single crystals at room temperature in the range 1000−1500 cm^{-1} with a Nicolet 740 FT-IR spectrometer equipped with a Nicolet Nic-Plan microscope. Raman spectra were recorded on single crystals at room temperature in the range 1050−1650 cm^{-1} with an optical multichannel analyser (OMARS 89, Dilor, France) equipped with a 1024 photodiode array detector and a cw Ar$^+$ laser ($\lambda_0 = 514.5$ nm). Raman spectra were obtained with the help of a microscope (100×) and the use of a low incident power laser (<10 mW) in order to minimize any local heating effect. UV−vis spectra were recorded at room temperature on pressed KBr pellets with a Perkin-Elmer 330 UV−vis spectrophotometer in the range 3820−25000 cm^{-1}.

Results and Discussion

Crystal Structures of α_1-$ET_8[CoW_{12}O_{40}]\cdot 5.5H_2O$ (I), α_1-$ET_8[FeW_{12}O_{40}]\cdot 9H_2O$ (II), α_2-$ET_8[CoW_{12}O_{40}]\cdot 0.5CH_3CN\cdot 3H_2O$ (III), and α_2-$ET_8[BW_{12}O_{40}]\cdot 2H_2O$ (IV). Only the structures of the Co^{II} and Fe^{III} derivatives of the α_1 phase, and of the Co^{II} and B^{III} derivtives of the α_2 phase have been solved.[23] The unit cell parameters of the other members of both α series have been determined either from single crystal X-ray analyses or from powder X-ray spectra (see Table 1). The stoichiometry

(16) North, A. C. T.; Philips, D. C.; Mathews, F. S. *Acta Crystallogr., Sect A* **1968**, *24*, 351.

(17) *International Tables for Crystallography*; Hahn, T., Ed.; D. Reidel Pub. Co.: Dordrecht, The Netherlands, 1983; Vol. A (Space Group Symmetry).

(18) MolEN, An Interactive Structure Solution Procedure. Enraf-Nonius, Delft, The Netherlands, 1990.

(19) Main, P.; Germain, G.; Woolfson, MULTAN-11/84, a System of Computer Programs for the Automatic Solution of Crystal Structures from X-Ray Diffraction Data. University of York, 1984.

(20) (a) Fuchs, J.; Thiele, A.; Palm, R. *Angew. Chem., Int. Ed. Engl.* **1982**, *21*, 789. (b) Sergienko, V. S.; Porai-Koshits, M. A.; Yurchenko, E. N. *J. Struct. Chem. (Engl. Transl.)* **1980**, *21*, 87. (c) Attanasio, D.; Bonamico, M.; Fares, V.; Imperatori, P.; Suber, L. *J. Chem. Soc., Dalton Trans.* **1990**, 3221. (d) Ouahab, L.; Bencharif, M.; Mhanni, A.; Pelloquin, D.; Halet, J. F; Peña, O.; Padiou, J.; Grandjean, D.; Garrigou-Lagrange, C.; Amiell, J.; Delhaès, P. *Chem. Mater.* **1992**, *4*, 666.

(21) Evans, H. T.; Pope, M. T. *Inorg. Chem.* **1984**, *23*, 501.

(22) (a) Robert, F.; Leyrie, M.; Hervé, G. *Acta Crystallogr.* **1982**, *B38*, 358. (b) Knoth, W. H.; Domaille, P. J.; Harlow, R. L. *Inorg. Chem.* **1986**, *25*, 1577. (c) Finke, R. G; Rapko, B.; Weakley, T. J. R.; *Inorg. Chem.* **1989**, *28*, 1573. (d) Weakley, T. J. R.; Evans, H. T.; Showell, J. S.; Tourné, G. F.; Tourné, C. M. *J. Chem. Soc., Chem. Commun.* **1973**, 139. (e) Evans, H. T.; Tourné, C. M.; Weakley, T. J. R. *J. Chem. Soc., Dalton Trans.* **1986**, 2699. (f) Wasfi, S. H.; Rheingold, A. L.; Kokoszka, G. F.; Goldstein, A. S. *Inorg. Chem.* **1987**, *26*, 2934. (g) Tourné, C. M.; Tourné, G. F.; Zonnevijlle, F. *J. Chem. Soc., Dalton Trans.* **1991**, 143. (h) Weakley, T. J. R.; Finke, R. G. *Inorg. Chem.* **1990**, *29*, 1235. (i) Finke, R.; Weakley, T. J. R. *J. Chem. Crystallogr.* **1994**, *24*, 123. (j) Gómez-García, C. J.; Borrás-Almenar, J. J.; Coronado, E.; Ouahab, L. *Inorg. Chem.* **1994**, *33*, 4016. (k) Gómez-García, C. J.; Coronado, E.; Gómez-Romero, P.; Casañ-Pastor, N. *Inorg. Chem.* **1993**, *32*, 3378.

(23) The structures of the B and Fe derivatives were solved in order to see if the different charges of the polyanions induce any influence on the structure. No noticeable differences were observed.

Table 2. Crystallographic Data for α_1-ET$_8$[CoW$_{12}$O$_{40}$]·5.5H$_2$O (**I**) α_1-ET$_8$[FeW$_{12}$O$_{40}$]·9H$_2$O (**II**), α_2-ET$_8$[CoW$_{12}$O$_{40}$]·0.5CH$_3$CN·3H$_2$O (**III**) and α_2-ET$_8$[BW$_{12}$O$_{40}$]·2H$_2$O (**IV**)

compound	**I**	**II**	**III**	**IV**
chem formula	C$_{80}$S$_{64}$H$_{75}$CoW$_{12}$O$_{45.5}$	C$_{80}$S$_{64}$H$_{82}$FeW$_{12}$O$_{49}$	C$_{81}$S$_{64}$H$_{71.5}$N$_{0.5}$CoW$_{12}$O$_{43}$	C$_{80}$H$_{68}$S$_{64}$O$_{42}$BW$_{12}$
a (Å)	13.971(9)	13.955(10)	16.66(2)	16.50(1)
b (Å)	43.117(7)	43.221(7)	43.42(2)	43.27(2)
c (Å)	14.042(5)	14.049(3)	12.14(1)	12.125(3)
β (deg)	107.25(3)	107.24(4)	111.78(9)	111.99(4)
V (Å^3)	8078	8093	8151	8026
Z	2	2	2	2
fw	6081.8	6141.7	6057.2	5970.5
space group	$I2/m$ (No. 5)	$I2/m$ (No. 5)	$I2/m$ (No. 5)	$I2/m$ (No. 5)
T (°C)	22	22	22	22
λ (Å)	0.71073	0.71073	0.71073	0.71073
ϱ_{calcd} (g·cm^{-3})	2.496	2.520	2.471	2.470
μ (cm^{-1})	96.544	96.270	95.656	96.150
R^a	0.068	0.060	0.061	0.065
R^b	0.102	0.073	0.078	0.094

[a] $R = \sum[||F_o| - |F_c||]/\sum|F_o|$. [b] $R_w = [\sum w(|F_o| - |F_c|)^2/\sum w|F_o|^2]^{1/2}$. $w = 4F_o^2/[\sigma^2(I) + (p|F_o|^2)^2]$.

and the general structure of both α phases are closely related, although they present some important differences (see below). The structure of the α_1 phase is quite similar to that described by Davidson et al. for the [SiW$_{12}$O$_{40}$]$^{-4}$ anion.[8a] Nevertheless, for the Si derivative the structure was solved in a noncentrosymmetric space group without solvent molecules.[24]

The general structure of both α_1 and α_2 phases is very similar: it consists of layers of the organic donors and the inorganic Keggin polyoxoanions perpendicular to the $\vec{b}$ axis (Figure 1a). The organic layers are formed by two different types of stacks that alternate in the [10$\bar{1}$] direction and run in the [101] direction (Figure 1b). One of the stacks (named II in Figures 1a and 2a) is formed by ET molecules packed in an eclipsed way while the other stack (named I in Figures 1a and 2a) is formed by dimers. These dimers are displaced along the central C=C bond by one external ring of the ET molecule so that there are six eclipsed S atoms between different dimers, giving rise to a zigzag chain of dimers (see Figure 1b).

In spite of the similarities between both α phases, some differences can be noted:

(i) The organic layers in the α_1 phase are formed by three crystallographically independent ET molecules (denoted as A, B, and C; there are four ET molecules of type A, two of type B, and two of type C per formula), whereas in the α_2 phase there are two different ET molecules (named A and B, with four ET molecules of each type per formula). In the α_1 phase the eclipsed stacks (II) are formed by alternated B and C type ET molecules, whereas in the α_2 phase all the molecules in II are of the B type. The dimerized chains (I) are exclusively formed by A type molecules in both phases.

(ii) The relative situation of the stacks in the organic layers is slightly different: if we consider the central dimerized stack as a reference (stack I$_0$ in Figure 2a), then, the α_2 phase can be obtained from the α_1 phase by displacing in one ET molecule (i.e., about 4.0 Å) the two neighboring dimerized chains in opposite directions along the stacking axis ("up" and "down" for stacks I$_{+1}$ and I$_{-1}$ in Figure 2a); type II chains remain unchanged in both α phases.
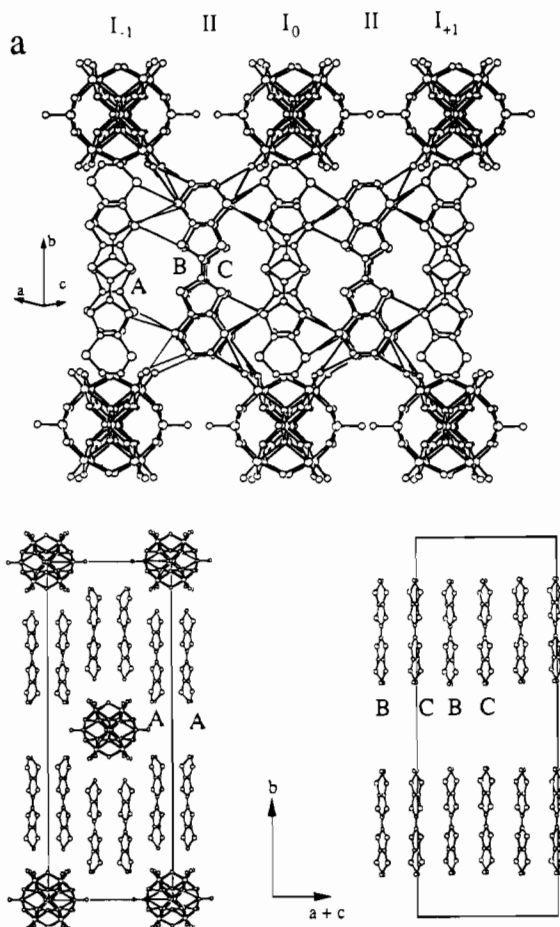
(24) For the above mentioned reasons, we have solved the structures in the centrosymmetric space group $I2/m$, but in order to be sure of the centrosymmetry of both α series we have tried to solve the structures in the acentric space group $I2$ (as the structure of the Si derivative was solved). In all cases we found that half of the atoms found in the Keggin unit, as well as those of the ET molecules, can be generated from the other half by simply applying a mirror plane, as has already been described by Evans and Pope in ref 21. We think it reasonable that both structures are, therefore, centrosymmetric.
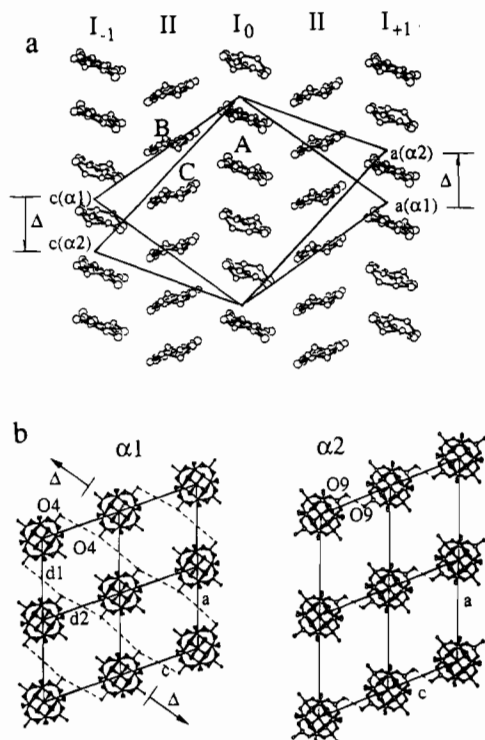

Figure 1. (a) Perspective view (ORTEP) of the layers in the ac plane of the structure of the α_1 series showing the shortest S$\cdots$S ($\leq$3.60 Å), S$\cdots$O ($\leq$3.20 Å), and C$\cdots$O ($\leq$3.20 Å) contacts between the organic and inorganic units. (b) Side view (ORTEP) of the dimerized (I) and eclipsed (II) stacks.

(iii) The displacement of the organic stacks is accompanied by a similar displacement of the inorganic anions (see Figure 2b). As can be seen in Figure 1b, the polyoxometalates lie in the holes left by two equivalent dimerized stacks of consecutive layers, so the displacement of the dimerized stacks are followed by the closer polyanions. That gives rise to the observed changes in the β angle and in the unit cell parameters a and c (in-plane anion–anion distances). Besides, the displacement in the inorganic sublattice results in a shortening of the distance between terminal oxygen atoms of neighboring anions (see

Figure 2. ORTEP projection in the ac plane showing the relationship between both α phases: (a) Organic layers; (b) inorganic layers showing the shortening of the terminal O···O distances O4···O4 ($d_1 = 7.95$ Å) and O9···O9 ($d_2 = 3.70$ Å).

Figure 3. Semilogarithmic plot of the dc resistivity (Ω cm) versus reciprocal temperature for the salts α_1-ET$_8$[SiW$_{12}$O$_{40}$] (full circles), α_1-ET$_8$[CoW$_{12}$O$_{40}$]·5.5H$_2$O (open squares) and α_2-ET$_8$[BW$_{12}$O$_{40}$]·2H$_2$O (open circles).

Figure 2b). This distance decreases from 7.95 Å in the α_1 phase to 3.70 Å in the α_2 phase. The *b* parameter is not affected, as the thickness of the layers is not changed, nor the unit cell volume (see Table 1). As the displacement of the dimerized stacks follows the direction of the stack ([101]), the dihedral angle between ET molecules of different stacks also remains unchanged (about 46°) in both α phases.

As in many other two dimensional radical salts of ET, the interstack distances are significantly shorter than the intrastack ones.[4] Thus, the shortest interchain S−S contacts are 3.41(2) Å, whereas the intrachain ones are 3.86(2) and 3.98(1) Å in the dimerized stacks (for the intra and inter dimers, respectively) and 4.04(2) Å in the regular stacks. Another important feature of this structure is the presence of short contacts between the organic and the inorganic layers. Thus, two kinds of interactions can be observed between the layers: the first one takes place between the S atoms of the eclipsed chains and some terminal O atoms of the polyoxoanions (shortest S−O distance of 3.15 (2) Å); the second one occurs via hydrogen bonds between several O atoms of the anions and the ethylenic groups of the ET molecules (shortest C−O distance of 3.13(3) Å).

Finally, there are two aspects in these new series worth to mention: (i) for all the Keggin polyanions it has been possible to selectively synthesize both α phases (except for the B and Si anions) by slightly changing the synthesis conditions. (ii) The stoichiometry is always 8:1 regardless of the anionic charges (from 4− to 6−). This feature has already been observed in the series of radical salts of TTF with the Keggin polyoxometalates [XM$_{12}$O$_{40}$]$^{(8-n)-}$ (X^{n+} = P^V, Si^{IV}; M = Mo, W), where the same structure is obtained[5c] for anionic charges of 3− and 4−. Moreover, the Keggin reduced polyanion [PMo$_{12}$O$_{40}$]$^{4-}$ presents the unit cell parameters of the α_1 phase,[8b] showing that Keggin polyoxomolybdates can also present these structures.[25] As a consequence of the various anionic charges, the averaged degrees of ionicity of the ET molecules may range from +1/2
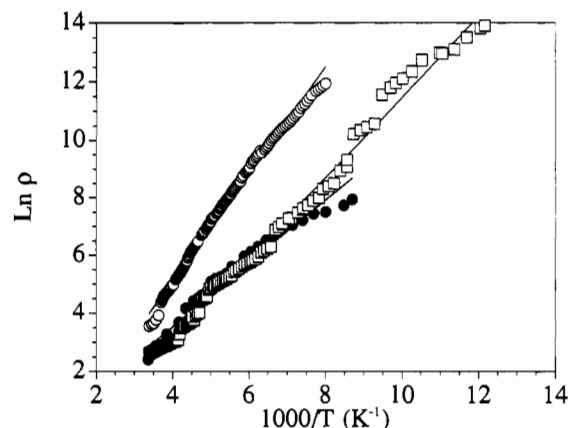
to +3/4. From the crystallographic data, using the known correlations[6a,26] between the central C=C bond distance and the degree of ionicity, we can roughly estimate that B and C types molecules are almost completely ionized whereas A type molecules are rather neutral. This charge distribution is also supported by a more complete relationship that also takes into account the central C−S bond distances of the TTF skeleton.[27] Nevertheless, the large standard deviations in the considered bond distances preclude any definite assignment. In order to obtain more precise information on this point we have carried out IR and Raman measurements; the results are presented in the corresponding section.

Electrical Properties. Only the Co^{II} and Si^{IV} members of the α_1 series, and the B^{III} salt of the α_2 series gave suitable single crystals for dc conductivity measurements. They are all semiconductors, with room temperature conductivities of 0.15, 0.07, and 0.03 S·cm^{-1}, and activation energies of 94, 119, and 159 meV for α_1-ET$_8$[SiW$_{12}$O$_{40}$], α_1-ET$_8$[CoW$_{12}$O$_{40}$]·5.5H$_2$O and α_2-ET$_8$[BW$_{12}$O$_{40}$]·2H$_2$O, respectively (see Figure 3).

Using a platelike single crystal of the salt α_1-ET$_8$[SiW$_{12}$O$_{40}$] we were able to measure the conductivity in different directions within the best developed face of the crystal (plane *ac*). The results showed that the anisotropy inside the plane is low (about 3:1), indicating the electronic two dimensional character of this kind of structure. This anisotropy is the same in order of that found in other ET radical salts.[4] Due to the similarity of the organic layers in both α phases, we can suggest that all the other salts of both series must behave in a similar way.

Transfer Integrals and Band Structure Calculations. The transfer integrals and the band structures have been evaluated by the dimer-splitting approximation[28] within the Extended Hückel Hamiltonian and using a double-ζ basis set.[29] The transfer integrals are reported in Figure 4. As discussed

(25) In fact, very recent studies with some Keggin-substituted polyoxometalates indicate that the series of anions [XM′(H$_2$O)M$_{11}$O$_{39}$]$^{-5}$, X = Si^{IV}, P^V; M′ = Ni^{II}, Mn^{II}, Co^{II}, Cu^{II}, Cr^{III}, Fe^{III}, ...; M = W^{VI}, Mo^{VI}) present the α$_2$ structure, except for the Mn^{II} derivative where a new α phase (α$_3$) appears: Galán-Mascarós, J. R.; Gimenez-Saiz, C.; Triki, S.; Gómez-García, C. J.; Coronado, E.; Ouahab, L. *Angew. Chem.*, in press.

(26) Ouahab, L.; Fettouhi, M.; Halet, J. F.; Yartsev, V. M.; Garrigou-Lagrange, C.; Delhaès, P.; Sourisseau, C. *New J. Chem.* **1993**, *17*, 399.

(27) Umland, T. C.; Allie, S.; Kuhlmann, T.; Coppens, P. *J. Phys. Chem.* **1988**, *92*, 6456.

(28) Ducasse, L.; Abderrabba, A.; Hoarau, J.; Pesquer, M.; Gallois, B.; Gaultier, J. *J. Phys. C: Solid State Phys.* **1986**, *19*, 3805.
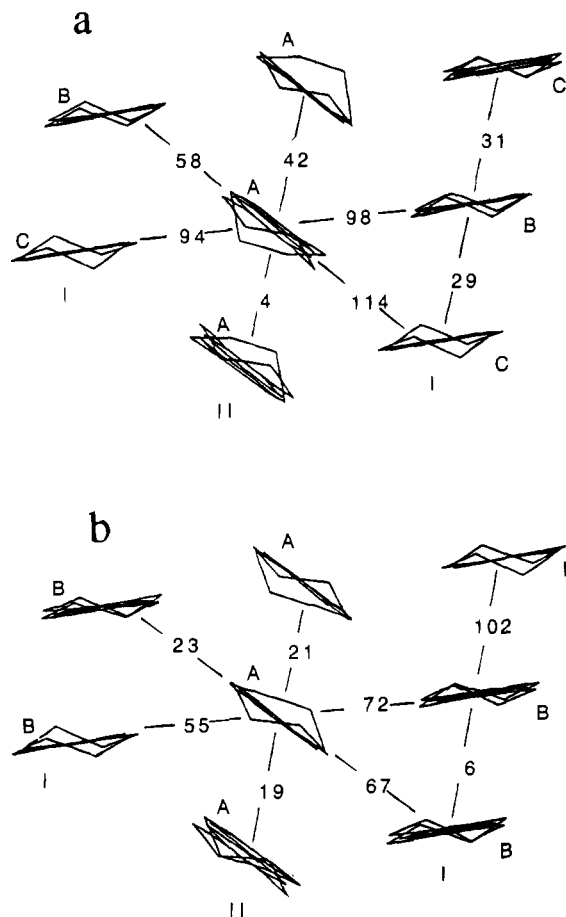
a

b

Figure 4. View of the *ac* layer with the transfer integrals found by EHT calculations (a) the α_1 phase and (b) the α_2 phase.

Table 3. Energies of the HOMO (eV) of the Independent Molecules for α_1- and α_2-ET$_8$[XW$_{12}$O$_{40}$]

ET molecule	α_1-Co	α_2-B
A	−8.722	−8.612
B	−8.380	−8.328
C	−8.351	

previously, for the α_1 series, the geometries of the B- and C-type molecules are rather similar while they differ from the geometry of A-type molecules. For the α_2 series, the geometries of the A- and B-type molecules are different. These observations are reinforced by the data concerning the HOMO energies ϵ which are reported in Table 3, where we observe: $\epsilon_A < \epsilon_B$ ($\approx\epsilon_C$). The differences in the HOMO energies have been taken into account in a relative scale for the calculation of the band structures: Figure 5a gives the calculated band structure for the $\{ET_8\}^{4+}$ layers in α_1-ET$_8$[CoW$_{12}$O$_{40}$]·5.5H$_2$O and Figure 5b gives the band structure for the formal $\{ET_8\}^{5+}$ layers in α_2-ET$_8$[BW$_{12}$O$_{40}$].

The calculated band structures are qualitatively different. Although the four lower energy bands build similar blocks in both compounds, the four upper bands exhibit different dispersion relations. This comes mainly from the ratio c3/c4: if one replaces the c3 and c4 integrals of α_2-B by their corresponding values in α_1-Co, the gap between the 6th upper band and the 7th one comes to zero. But the main difference between the band structures of the two salt arises from the band filling. It is
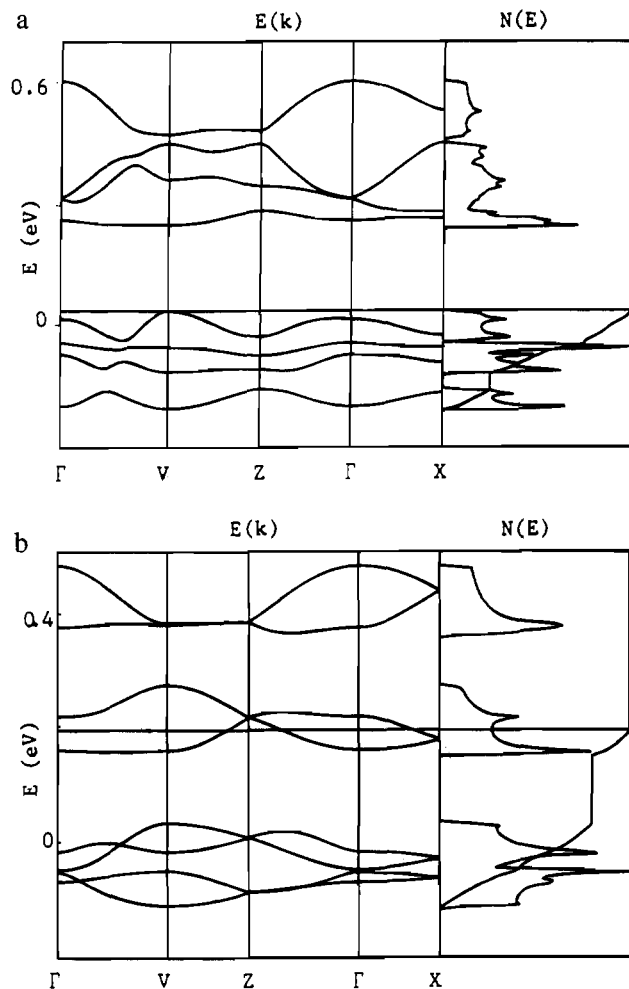
(29) (a) Ducasse, L.; Fritsch, A. *Solid State Commun.* **1994**, *91*, 201. (b) Whangbo, M.-H.; Williams, J. M.; Leung, P. C. W.; Beno, M. A.; Emge, T. J.; Wang, H. H.; Carlson, K. D.; Crabtree, G. W. *J. Am. Chem. Soc.* **1985**, *107*, 5815.
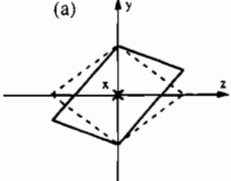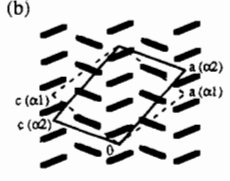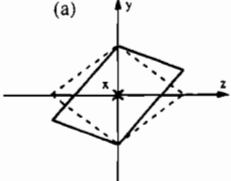
a

b

Figure 5. Dispersion energy $E(k)$ and density of states $N(E)$: (a) the ET$_8^{4+}$ layers in α_1-ET$_8$[CoW$_{12}$O$_{40}$]·5.5H$_2$O; (b) the ET$_8^{5+}$ layers in α_2-ET$_8$[BW$_{12}$O$_{40}$]·2H$_2$O.

clear from Figure 5 that a semimetallic character is predicted for α_2-B by the one-electron approach while a semiconducting behavior is found for α_1-Co (the energetic gap should be close to 200 meV).

On the basis of these calculations, we can try to explain the observed semiconducting behavior of these salts. We learn from the band structure that the results for α_1-Co apparently agree with the experimental data. However, it is important to notice that the gap of 200 meV found in that case is directly related to the difference in the HOMO energies of the ET molecules (see Table 3). If one turns this difference to zero, the corresponding band structure now corresponds to a semimetallic character. In the case of the α_2-B salt, there is a qualitative disagreement. The difference in the HOMO energies does not lead to a semiconducting character because of the band filling which now corresponds to an average charge of $^5/_8$ + per molecule. The origin of the semiconducting behavior in that case is certainly related to the existence of different molecules with different geometries and different site energies. The EH approach which does not include self-consistently the effects of the charge on the electronic picture is, thus, unable to give a correct description of the metallic vs insulating character. There is a whole of experimental and theoretical data showing that the molecules bear different charges. The semiconducting state might be related to some kind of site localization. In contrast, the α-ET$_2$-[MHg(SCN)$_4$] (M = K$^+$ and NH$_4^+$) salts show a very similar crystal structure but with a different space group so that the

unit cell contains four ET molecules.[30] Moreover, as for the α_1 phase, there are three crystallographically independent molecules but their geometries and HOMO energies are quite similar in that case, in agreement with the metallic character (there, the $3/4$-filled band system agrees with its metallic state).

Optical Properties. The UV−vis spectra show for all the salts a large band of type A (corresponding to electronic transfers between neutral and completely charged ET molecules)[31] at around 4000 cm^{-1}, indicating the existence of a mixed-valence state in the organic donors, as well as a band of type B (corresponding to electronic transfers between completely ionized ET molecules)[32] at about 10 000−12 000 cm^{-1}.

Each ET molecule is nearly flat and approximately keeps the D_{2h} symmetry. We assumed, as in other studies,[33] that the ET dimers maintain the D_{2h} symmetry in spite of the distortion of the individual molecules. The ET molecule contains two types of double bonds; we shall focus on the ν_2 (ν(C=C, central), a_g), ν_3 (ν(C=C, ring), a_g), and ν_{27} (ν(C=C, ring), b_{1u}) modes as their wavenumbers are known to be sensitive to the electronic character of the donor molecules and, thus, they may provide a direct information about the degree of ionicity (ϱ). Under the isolated dimer approximation, one expects two ν(C=C) Raman-active vibrations: $2a_g$ (only one IR-active: $1b_{1u}$), and in the crystalline state, owing to the site and correlation effects, there must be six Raman-active (also six IR-active) vibrations for the ET molecules in general positions (A-type in both α phases and B-type in the α_2 phase), four Raman-active (two IR-active) vibrations for the molecules on a center of inversion (B-type molecules in the α_1 phase) and three Raman-active (also three IR-active) vibrations for the molecules on the two-fold axis (C-type molecules in the α_1 phase). Thus, from symmetry considerations for the ν_2, ν_3, and ν_{27} modes one can deduce the existence of up to 13 Raman active (11 IR-active) vibrations for the α_1 phase and up to 12 Raman-active (also 12 IR-active) vibrations for the α_2 phase (see Table 4).

The IR spectra of all these salts are very similar, confirming the presence of the same type of stacks in all the salts, except in the 1000−400 cm^{-1} region where small differences due to the different polyanions are observed (see Table 5). In all the spectra the A band is also observed as a large and intense band centered at 3500−4200 cm^{-1} (see Figure 6). The main band wavenumbers and their assignments[34] for both the ET molecules and the anions are listed in table 5. In general, the bands of the ET molecules are very similar to those found in other completely ionized ET$^+$ radical cations,[35] suggesting the presence of almost completely charged ET molecules. Nevertheless, the additional presence of almost neutral ET molecules cannot be inferred from the IR spectra as these ET molecules would give rise to very weak bands[36] for the modes characteristic of the degree of ionicity (ν_2, ν_3, and ν_{27}). Spectra recorded at 12 K on samples of both phases (the Co^{II} derivative of the α_1 phase and the B^{III} derivative of the α_2 phase) do not show the presence of new bands nor important shifts as compared to room

(30) Mori, H.; Tanaka, S.; Oshima, M.; Saito, G.; Mori, T.; Murayama, Y.; Inokuchi, H. *Bull. Chem. Soc. Jpn.* **1984**, *57*, 627.
(31) Torrance, J. A.; Scott, B. A.; Welber, F. B. *Phys. Rev. B* **1979**, *19*, 730.
(32) Delhaès, P.; Garrigou-Lagrange, C. *Phase Transitions* **1988**, *13*, 87.
(33) Swietlik, R.; Garrigou-Lagrange, C.; Sourisseau, C.; Pages, G.; Delhaès, P. *J. Mater. Chem.* **1992**, *2*, 857.
(34) The assignment have been made following the nomenclature of ref 33 with the interpretations of ref 6a and 35.
(35) Kozlov, M. E.; Pokhodnia, K. I.; Yurchenko, A. A. *Spectrochim. Acta* **1989**, *45A*, 437.
(36) Moldenhauer, J.; Horn, Ch.; Pokhodnia, K. I.; Schweitzer, D.; Heinen, I.; Keller, H. J. *Synth. Met.* **1993**, *60*, 31.

Table 4. Correlation Tables for the ν(C=C) Stretching Modes in Both α Phases with (a) the Molecular Axis Notation and (b) a Sketch of the Unit Cell in the *ac* Plane

temperature results, precluding any possible identification of the almost neutral ET molecules.[37]

The only significant differences in the IR spectra appear in the 1000−400 cm^{-1} region, corresponding to the Keggin polyanion vibrations. Thus, we note that the band corresponding to the W−O$_a$ (terminal) bond (which appears at 939−967 cm^{-1}) gives a good idea of the anionic charge of the Keggin polyanion:[38] for the ET$_8$[XW$_{12}$O$_{40}$] salts with X = 2(H$^+$), Co^{II}, and Cu^{II} (anionic charge of 6−), the mentioned band appears at 939−947 cm^{-1}, whereas for X = B^{III} and Fe^{III} (anionic charge of 5−), this band appears at 951 cm^{-1} and for X = Si^{IV} (anionic charge of 4−), it appears at 967 cm^{-1}. This observation confirms that these salts present the highest charged anions ever used in this type of radical salts (up to 6−). The other differences, as expected, come from the X−O bonds (see Table 5).

In order to get a more precise knowledge of the electronic distribution in the organic sublattice, we have performed Raman scattering measurements on the Cu^{II} and Si^{IV} derivatives of the α_1 phase and on the Co^{II}, 2(H$^+$), and B^{III} derivatives of the α_2 phase.

Although the Raman signals are broad and, in some cases, appear just like shoulders, up to 12 bands can be observed for the different orientations of the single crystals. These 12 bands are, within experimental error, in the same positions for all the salts, indicating that the electronic distribution in the organic lattice must be very similar in all cases. As an illustrative example we show in Figure 7 four distinct polarized Raman spectra recorded for the α_2-Co derivative. As already ob-

(37) We have also performed IR spectra on single crystals at room temperature for several compounds of both phases in the 1500−1000 cm^{-1} region. They are all very similar and we do not observe any significant difference compared to those obtained in KBr pellets.
(38) Rocchiccioli-Deltcheff, C.; Thouvenot, R.; Franck, R. *Spectrochim. Acta* **1976**, *32A*, 587.

Table 5. Infrared Band Wavenumbers (cm^{-1}) and Assignments in the Series α_1- and α_2-ET$_8$[XW$_{12}$O$_{40}$], with Values in Parentheses at $T = 12$ K

assignment	α_1-Co	α_1-Cu	α_1-H$_2$	α_2-Co	α_2-Cu	α_2-H$_2$	α_1-Fe	α_2-B	α_1-Si
A	3850 (3850)	3950	4050	3850	4250	3800	3900	3450 (3450)	4000
ν(CH$_2$)	2964 (2962)	2963	2963	2966	2963	2964	2965	2968 (2967)	2968
ν(CH$_2$)	2926 (2916)	2927	2928	2923	2926	2919	2924	2926 (2913)	2925
ν(CH$_2$)	2873 (2846)	2871	2870				2873		
ν_{27}	1447 (1451)	1449	1451	1447	1449	1450	1451	1447 (1450)	1447
$\nu_2 + \delta$(CH$_2$)	1407 (1409)	1407	1409	1406	1405	1405	1409	1406 (1410)	1406
						1384	1385	1381 (1379)	
ν_3	1345 (1346)	1344	1346	1344	1344	1346	1344	1345 (1346)	1346
ν_{29}	1282 (1282)	1282	1283	1282	1283	1284	1282	1284 (1284)	1284
ν_{46}	1261 (1263)	1260	1262	1262	1260	1262	1260	1261 (1261)	1261
ν_{67}	1171 (1171)	1170	1170	1169	1170	1170	1172	1172 (1171)	1173
ν_{38}	1129 (1131)	1128	1129	1128	1128		1126	1128 (1131)	1128
ν_{47}	1122 (1120)	1123	1121	1122	1121	1121	1122	1123 (1121)	1122
	1048 (1029)					1048	1041		1047
ν_{30}	1016 (1018)	1016	1015	1014	1016	1018	1019	995 (995)	1015
H$-$O^a			954			956			
W$=$O^d	941 (942)	943	945	939	941	947	951	951 (954)	967
Si$-$O^a									917
W$-$O$^c-$W	870 (869)	873	881	868	870	877	873	898 (898)	881
								821 (819)	
W$-$O$^b-$W	757 (754)	759	786	754	757	777	773	775 (773)	796
ν_{33}	689 (691)	682	681	691	685	682	723	682 (683)	679
ν_{51}	643 (643)	643	644	642	644	642	645	643 (644)	646
δ(O$^a-$Si$-$O^a)								530 (532)	533
ν_9	474 (476)	474	475	471	471	472	466	474 (476)	475
δ(O$^a-$M$-$O^a)	452 (455)	440	421	452	443	421	452	389 (390)	386
			403			403			
ν_{35}	394 (395)	398	378	393	393	378	394		

^{a} Tetrahedral. ^{b} Corner sharing. ^{c} Edge sharing. ^{d} Terminal.
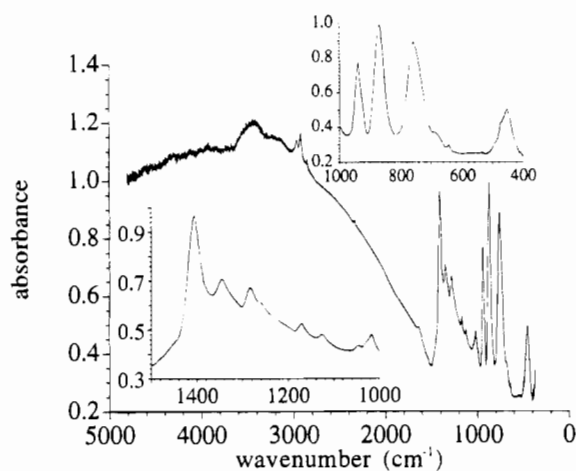
Figure 6. IR spectrum of the α_1-ET$_8$[CoW$_{12}$O$_{40}$]·5.5H$_2$O salt. The 1500$-$1000 and 1000$-$400 cm^{-1} regions are detailed in the insets.

served,[39] the bands can be grouped into Davydov's doublets which are split by approx. 20 cm^{-1}. The wavenumbers of these twelve bands, as well as the central values of the six doublets, are reported in Table 6. If we consider that only the modes ν_2, ν_3, and ν_{27} are observed in the mentioned region, there must be two doublets coming from each mode; i.e., a maximum of three doublets should be observed if all the ET molecules behave in the same way. Nevertheless, we observe up to six doublets, in agreement with the idea that there are two types of differently charged ET molecules. Moreover, from the linear relationships found in other ET salts[33,40] between the wavenumbers of the ν_2, ν_3, and ν_{27} modes and the degree of ionicity (ϱ), we can estimate ϱ for the ET molecules. Thus, if we assign the doublets

centered at 1524 and 1459 cm^{-1} to the ν_2 mode, those centered at 1482 and 1438 cm^{-1} to the ν_3 mode, and those centered at 1417 and 1397 cm^{-1} to the ν_{27} mode,[41] we can estimate by interpolation ϱ values of about 0.8$-$0.9 and about 0.2 for the two kinds of ET molecules (see Figure 8). This estimation is displayed in Table 6. The total charge calculated for the ET molecules per anion would be then of about 4, in all cases.

Magnetic Properties. The static magnetic susceptibility of the salts containing non magnetic anions (X = 2(H$^+$), B^{III}, Si^{IV}) exhibits a shoulder in χ_m around 60 K and a paramagnetic Curie tail at lower temperatures. The plot of the $\chi_m T$ product vs T shows, for the three salts, a continuous decrease on lowering the temperature from a value of about 1.5 emu·K·mol^{-1} for X = 2(H$^+$) and Si^{IV}, and 2.0 emu·K·mol^{-1} for the B^{III} salt at room temperature, to a value around 0.1$-$0.2 emu·K·mol^{-1} at low temperatures (Figure 9a). The salts containing paramagnetic metals inside the Keggin anion (X = Co^{II}, Cu^{II} and Fe^{III}) show a decrease in the $\chi_m T$ product similar to that observed for the salts containing diamagnetic anions, reaching, at low temperatures, the value of the corresponding magnetic ion (Figure 10). We note that, for a given salt, the behavior is the same in both α phases.

For those salts with non magnetic anions, we can subtract a Curie tail contribution estimated from the $1/\chi_m$ vs T plot at low temperatures (Table 7). The so corrected susceptibility data (χ_{cor}) present a round maximum at about 60 K for the three salts (Figure 11), which indicates the existence of an antiferromagnetically coupled low dimensional lattice. In view of the structural and electronic characteristics of the organic network, a tentative way to explain the above magnetic behavior may consist in assuming the coexistence of a highly localized spin chain antiferromagnetically coupled and a delocalized mixed-valence one (eclipsed (type II) and dimeric (type I) stacks,

(39) Sugai, S.; Mori, H.; Yamochi, H.; Saito, G. *Phys. Rev. B* **1993**, *47*, 14374.

(40) Hau Wang, H.; Ferraro, J. R.; Williams, J. M.; Geiser, U.; Schlueter, A. *J. Chem. Soc., Chem. Commun.* **1994**, 1893.

(41) The ν_{27} modes are assigned by elimination and taking into account that this mode must give rise to less intense bands compared to those of the other modes.
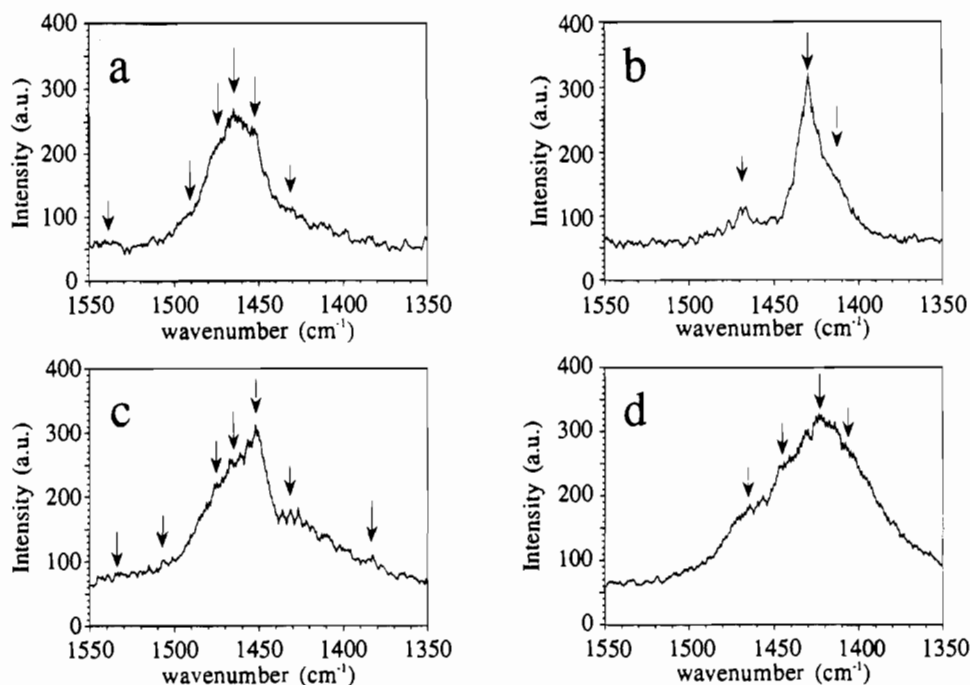
Figure 7. Polarized Raman spectra of the α_2-ET$_8$[CoW$_{12}$O$_{40}$] salt when the polarization vector is in the *ac* plane (a and b), perpendicular to the *b* axis (c), and parallel to it (d). The arrows indicate the positions of the bands.

Table 6. Wavenumbers (cm^{-1}) and Assignments of the Raman Modes and Interpolated Degrees of Ionicity for the series α_1- and α_2-ET$_8$[XW$_{12}$O$_{40}$]

wavenumber	avdg value	mode $(\varrho)^a$	mode $(\varrho)^b$
1540	1524	ν_2 (0.27)	ν_2 (0.17)
1508			
1489	1482	ν_3 (0.17)	ν_3 (0.29)
1475			
1465	1459	ν_2 (0.94)	ν_2 (0.93)
1453			
1445	1438	ν_3 (0.87)	ν_3 (0.79)
1431			
1421	1417	ν_{27} (0.21)	
1413			
1404	1397	ν_{27} (0.93)	
1390			

^{a} After the equations: $\nu_2 = 1550 - 97\varrho$; $\nu_3 = 1493 - 63\varrho$ and $\nu_{27} = 1423 - 28\varrho$ from ref 33. ^{b} After the equations: $\nu_2 = 1539 - 86\varrho$ and $\nu_3 = 1508 - 88.4\varrho$ from ref 40.

respectively). Thus, we fit the corrected magnetic susceptibility (χ_{cor}) to eq 1, where the first term is the equation developed

$$\chi_{cor} = \left(\frac{\mu_B N_A g^2 n_1}{kT}\right) \times$$

$$\left(\frac{0.25 + 0.14995\left(\frac{J_1}{T}\right) + 0.30094\left(\frac{J_1}{T}\right)^2}{1 + 1.9862\left(\frac{J_1}{T}\right) + 0.68854\left(\frac{J_1}{T}\right)^2 + 6.0626\left(\frac{J_1}{T}\right)^3}\right) +$$

$$\left(\frac{\mu_B N_A 8 g^2 n_2}{kT}\right)\left(\frac{1}{3 + \exp\left(\frac{J_2}{T}\right)}\right) \quad (1)$$

by Hall and Hattfield for a regular antiferromagnetic chain[42] from the numerical results of Bonner and Fisher[43] and the second

(42) Brown, D. B.; Donner, J. A.; Hall, J. W.; Wilson, S. R.; Wilson, R. B.; Hodgson, D. J.; Hatfield, W. E. *Inorg. Chem.* **1979**, *18*, 2635.
(43) (a) Bonner, J. C.; Fisher, M. E.; *Phys. Rev.* **1964**, *135*, A640. (b) Eggert, S.; Affleck, I.; Takahashi, M. *Phys. Rev. Lett.* **1994**, *73*, 332.
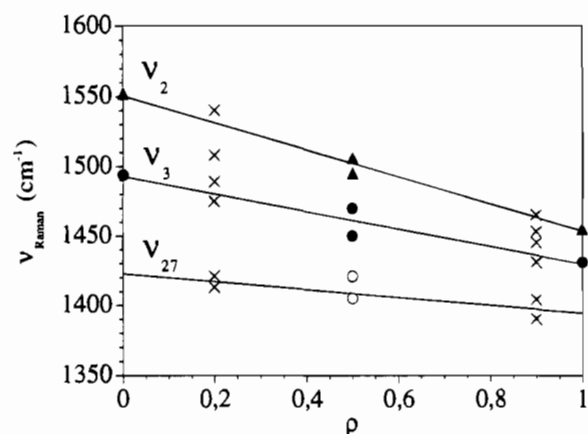

Figure 8. Correlation of the ν_2 (full triangles), ν_3 (full circles) and ν_{27} (open circles) Raman wavenumbers with the oxidation state of various ET salts. Continuous lines are the least squares fit from ref 33. The crosses are the values found in the title compounds (see Table 6).

term accounts for an activated magnetic contribution coming from the dimeric chain. J_1 and J_2 are the exchange parameters for the chain and the dimer, respectively, and n_1 and n_2 are the number of spins in each system. This model gives good agreement with the experimental corrected susceptibilities for J_1 values of ≈ -60 cm^{-1} (the exchange Hamiltonian is written as $-J_1\sum s_i s_j$), which accounts for the maximum in χ_{cor} and a singlet–triplet energy gap, J_2, of about -300 cm^{-1} (continuous lines in Figure 11). Table 7 displays the values of the Curie-type corrections as well as the values obtained for the J_1, J_2, n_1, and n_2 parameters. The values obtained for n_1 and n_2 (the number of spins on the localized and dimerized chain, respectively) indicate that in the localized (eclipsed) chain each ET molecule (B and C type) has a degree of ionicity of about 0.7, whereas the ET molecules of the dimerized chain (A type) bear a charge of about 0.2 (0.5 in the B salt), in good agreement with the Raman findings. These results indicate that the number of unpaired spins is 4 in the 2(H$^+$) and Si^{IV} salts (regardless of the different anionic charge of the anions: 6$-$ and 4$-$, respectively), and is, instead, 5 in the B^{III} salt.
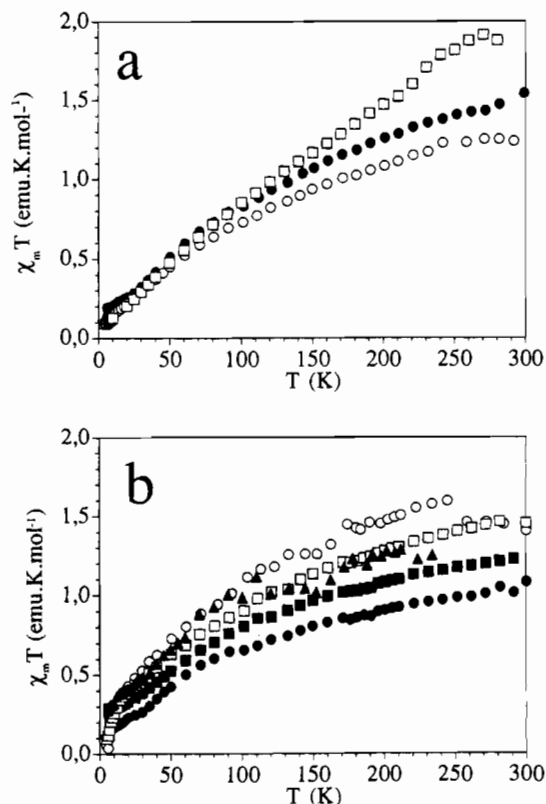
Figure 9. Plot of the $\chi_m T$ product vs T: (a) the ET radical salts containing diamagnetic anions α_1-ET$_8$[SiW$_{12}$O$_{40}$] (full circles), α_2-ET$_8$-[H$_2$W$_{12}$O$_{40}$] (open circles) and α_2-ET$_8$[BW$_{12}$O$_{40}$]·2H$_2$O (open squares); (b) the organic sublattice of the salts α_1-ET$_8$[CoW$_{12}$O$_{40}$] (open squares), α_2-ET$_8$[CoW$_{12}$O$_{40}$] (open circles), α_1-ET$_8$[CuW$_{12}$O$_{40}$] (full squares), α_2-ET$_8$[CuW$_{12}$O$_{40}$] (full circles), and α_1-ET$_8$[FeW$_{12}$O$_{40}$] (full triangles).
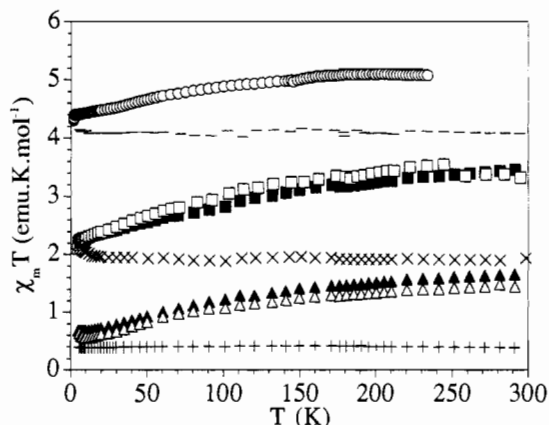

Figure 10. Plot of the $\chi_m T$ product vs T for the ET radical salts containing paramagnetic anions α_1-ET$_8$[CuW$_{12}$O$_{40}$] (full triangles), α_2-ET$_8$[CuW$_{12}$O$_{40}$] (open triangles), α_1-ET$_8$[CoW$_{12}$O$_{40}$] (full squares), α_2-ET$_8$[CoW$_{12}$O$_{40}$] (open squares), and α_1-ET$_8$[FeW$_{12}$O$_{40}$] (open circles). The tetrabutylammonium salts of the corresponding magnetic polyanions are also shown: [CuW$_{12}$O$_{40}$]$^{6-}$ (+), [CoW$_{12}$O$_{40}$]$^{6-}$ (×), and [FeW$_{12}$O$_{40}$]$^{5-}$ (—).

The values found for the J_1 parameter are not far from those estimated from the transfer integrals, t, calculated by EHT ($J \approx \alpha t^2/U$, with $1 < \alpha < 2$ and $U \approx 1$ eV).[44] Nevertheless, the non existence up to date of a triangular bidimensional model with different exchange parameters precludes the possibility of obtaining any exact set of exchange parameters comparable to that deduced from EHT.

The presence of such a Curie tail at low temperatures in the salts with non magnetic anions has also been found[8b] in the isostructural compounds of the α_1 series with the anions [SiW$_{12}$O$_{40}$]$^{4-}$ and [PMo^{V}Mo$^{VI}_{11}$O$_{40}$].$^{4-}$ This result is also reminiscent of charge ordering in heavy fermion compounds.[45] This type of paramagnetic contribution has also been found quite often in one dimensional organic conductors as for example in TCNQ charge transfer salts.[46] Several explanations have been proposed as the presence of defects inside a given stacking, this is the so called interrupted strand model,[47] or the electronic correlations in a 1-d disordered Hubbard model.[48] However, it appears that such a Curie tail as observed in these compounds cannot be explained by these arguments because its value is about 1 order of magnitude larger than observed previously in quasi 1-d systems.

A possible explanation would be the presence of very narrow electronic bands as postulated a long time ago by Kommandeur et al.[49] who have demonstrated that in a nondegenerated electronic gas a magnetic localization can occur, giving rise to a strong Curie component of the spin susceptibility. However, this model is not realistic because non interacting electrons are considered, and it is well-known that in these compounds we are in the presence of rather strong electronic correlations. Such a model has been proposed by Kaplan et al.[50] These authors have shown that in a narrow band width (W) of a correlated gas ($W \approx U$), the electronic states can be either singly or doubly occupied. In such a situation, a strong Curie component should appear, as also discussed in Mott's book, where this effect is associated with some disorder. In our case, the presence of the Curie tail in all compounds of the series could be associated with the very anisotropic charge distribution. Thus, we can imagine that at low temperatures the slow electron hopping in the dimeric chain leads to a localization of the spins at low temperatures in such a way that a significant part of the spins are isolated in the dimeric chains (while the rest are on two adjacent ET molecules and contribute to the singlet to triplet energy term). This simple idea is in agreement with the decrease in the number of unpaired electrons in the B compound compared with the Si and 2(H$^+$) ones; in the former case, the presence of one electron more in the dimeric chain reduces the number of isolated spins, increasing the number of dimers.

For those salts containing magnetic polyanions, the magnetic moment of the salts corresponds to the simple addition of the contributions of the magnetic Keggin anions with that of the organic sublattice. This observation indicates that both sublattices do not interact significantly, despite the fact that short contacts between the organic and inorganic parts are present in the structure. Once subtracted the magnetic moment of the anion, the contribution of the organic sublattice is similar to that obtained in the salts with diamagnetic anions (see Figure 9b), i.e., the ET molecules are antiferromagnetically coupled independently of the magnetic polyanions. This result can be easily understood if we realize that the central magnetic centers are quite well isolated in the central tetrahedral cavity of the Keggin anion.

Electron Spin Resonance. Single crystals suitable for the ESR study have been obtained for X = Si^{IV}, Cu^{II}, and Co^{II} in

(44) U is the intrasite coulombic term: Pincus, P. *Solid State Commun.* **1972**, *11*, 305.

(45) Bonville, P.; Ochiai, A.; Suzuki, T.; Vincent, E. *J. Phys. I* **1994**, *4*, 595.
(46) Aly, F.; Flandrois, S.; Delhaès, P.; Dupuis, P. *Solid State Commun.* **1973**, *12*, 1099.
(47) Bloch, A. N.; Varma, C. M.; *J. Phys. C., Solid State Physics* **1973**, *6*, 1849.
(48) Theodorou, G.; Cohen, M. H. *Phys. Rev. Lett.* **1976**, *37*, 1014.
(49) Fedders, P. A.; Kommandeur, J. *J. Chem. Phys.* **1970**, *52*, 2014.
(50) Kaplan, T. A.; Mahanti, S. A.; Hartmann, W. M. *Phys. Rev. Lett.* **1971**, *27*, 1796.

Table 7. Magnetic Parameters for the Diamagnetic Derivatives of the Salts α_1- and α_2-ET$_8$[XW$_{12}$O$_{40}$]^a

phase-X	C	n_{para}	n_1	n_2	$-J_1$ (cm^{-1})	$-J_2$ (cm^{-1})	n_{tot}	ϱ_{chain}	ϱ_{dim}
α_1-Si	0.130	0.35	2.86	0.79	64	311	4	0.72	0.20
α_2-H$_2$	0.105	0.28	2.82	0.90	64	356	4	0.71	0.23
α_2-B	0.037	0.10	2.80	2.20	56	313	5	0.70	0.55

^{a} n_1 and n_2 are the number of electrons per formula on the regular and dimeric chains, respectively. n_{para} is the deduced number of electrons giving rise to the paramagnetic Curie tail (C). n_{tot} is the total number of unpaired electrons per formula.
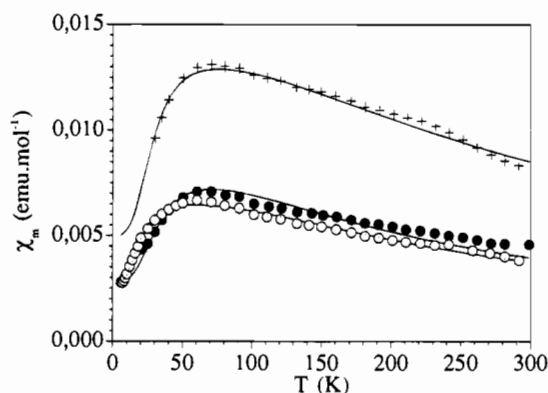

Figure 11. Plot of χ_{cor} vs T for the salts α_1-ET$_8$[SiW$_{12}$O$_{40}$] (full circles), α_2-ET$_8$[H$_2$W$_{12}$O$_{40}$] (open circles), and α_2-ET$_8$[BW$_{12}$O$_{40}$] (crosses). Continuous lines are the best fits to the model (see text).

the α_1 series and for X = B^{III}, Co^{II} and Fe^{III} in the α_2 series. For the salts containing nonmagnetic anions (X = B^{III} and Si^{IV}), the room temperature ESR spectra are characterized by a single Lorentzian signal. The angular dependences of the line width (ΔH), and of the g factor have been measured taking a^* (ω rotation), b (ϕ rotation) and c^* (ψ rotation) as rotation axes, where a^* and c^* lie in the crystallographic ac plane (which is parallel to the best developed face of the crystal) and are perpendicular to each other and to the b axis (see inset of Figure 14). For the ω and ψ rotations the angular dependence of both ESR parameters is very similar: they show a maximum at $\theta = 90°$, corresponding to the orientation where the external magnetic field, H_0, is parallel to the b axis (and, thus, to the central C=C double bond). The angular dependences of ΔH and g for the three rotations of the B salt are shown in parts a and b of Figure 12 (the Si salt shows very similar angular dependences of both ESR parameters). If we assume that the ET layers show axial symmetry, we can fit the behavior of ΔH and g for both salts to the classical equations:[6e,51]

$$g_{obs}^2 = g_{\parallel}^2 \sin^2\theta + g_{\perp}^2 \cos^2\theta \tag{2}$$

$$\Delta H_{obs}^2 = \Delta H_{\parallel}^2 \sin^2\theta + \Delta H_{\perp}^2 \cos^2\theta \tag{3}$$

The values found for ΔH and the g factor along the three rotation axes are listed in Table 8. The g values, which are molecular characteristics,[4] are very similar in both salts and similar to those found in other α phases,[52] but in the Si salt, ΔH varies from 38 to 22−26 G, whereas in the B^{III} salt these values are higher (from 63 to 36−43 G).

The values found when H_0 is in the ac plane are very similar indicating that the anisotropy in this plane is very small, as could be expected from the crystal structure. The higher value of ΔH for the B compound compared to that of the Si one suggests that the electronic dimensionality of the first salt is higher. As has been established, the relaxation rates increase with the
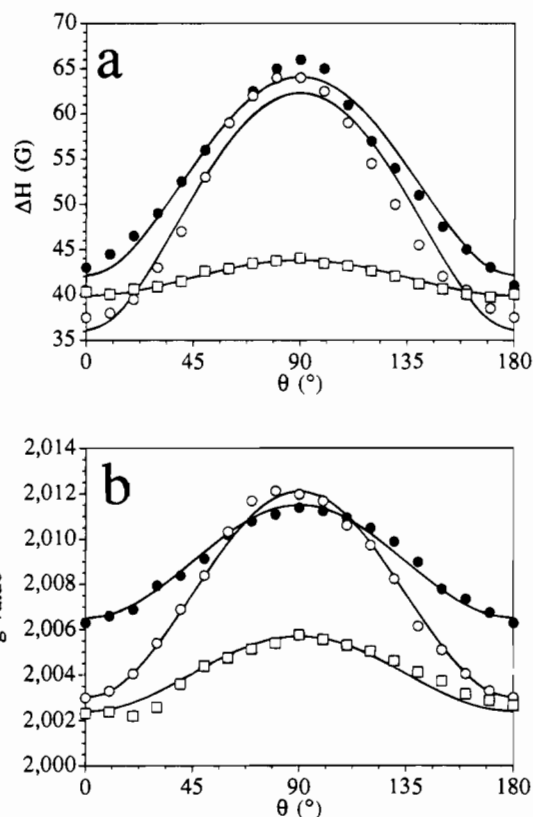

Figure 12. Angular dependence of (a) the line width (ΔH) and (b) the g factor at room temperature for the salt α_2-ET$_8$[BW$_{12}$O$_{40}$] for the ω (full circles), ψ (open circles), and ϕ (open squares) rotations. Continuous lines are the best fits to the equation indicated in the text.

effective dimensionality;[4] thus, a broadening of the ESR line width is predicted when more two dimensional electronic systems are realized.

The thermal variations of ΔH and g in the temperature range 4.2−300 K have been recorded with the magnetic field parallel to the central C=C bond of the ET molecules (b axis). In the two salts ΔH smoothly decreases with the temperature, and for $T < 100$ K it decreases more sharply to reach a value of $\approx$10 G at 4.2 K, when the Curie component is present. The g factors remain nearly constant in the investigated temperature range (Figure 13). The thermal dependence of the spin susceptibility calculated from the ESR spectra follows the behavior observed by static susceptibility measurements.

The room temperature ESR spectra of the salts containing paramagnetic anions (X = Co^{II}, Cu^{II}, and Fe^{III})[53] show larger signals than those of their diamagnetic congeners (maximum values of 85−95 G compared to 38−66 G in the diamagnetic salts, see Table 8). On the contrary, the g values do not show any significant difference. The angular variation of ΔH and g is also similar to that observed in the salts of diamagnetic anions, with maximum values of these parameters along the b axis. Nevertheless, it is important to note that the behavior of the g

(51) (a) Sugano, T.; Saito, G.; Kinoshita, M. *Phys. Rev. B* **1986**, *34*, 117. (b) Sugano, T.; Saito, G.; Kinoshita, M. *Phys. Rev. B* **1987**, *35*, 6554.
(52) Fettouhi, M.; Ouahab, L.; Grandjean, D.; Ducasse, L.; Amiell, J.; Canet, R.; Delhaès, P. *J. Mater. Chem.*, in press.

(53) For the [CoW$_{12}$O$_{40}$]$^{6-}$ anion we have not observed any important difference in the EPR spectra of both α phases.

Table 8. ESR Room Temperature Parameters (g Value and Peak to Peak Line Width, ΔH, in G) for Single Crystals of Different Compounds in the Series α_1- and α_2-ET$_8$[MW$_{12}$O$_{40}$] Obtained from the Fit of ΔH and g to Eqs 2 and 3 in the Text (Values in Parentheses Are the Standard Deviations in the Last Digits)

phase-X	α_1-Co	α_1-Cu	α_2-Co	α_2-Fe	α_1-Si	α_2-B
g_{max}	2.0082(1)	2.0100(1)	2.0072(1)	2.0114(2)	2.0099(1)	2.0118(1)
g_{med}	2.0059(1)	2.0049(1)	2.0052(1)	2.0031(2)	2.0059(1)	2.0061(1)
g_{min}			2.0027(1)		2.0030(1)	2.0027(1)
ΔH_{max}	95(1)	94(1)	83(1)	87(1)	38(1)	63(1)
ΔH_{med}	80(1)	76(1)	73(1)	62(1)	26(1)	43(1)
ΔH_{min}			53(1)		22(1)	36(1)
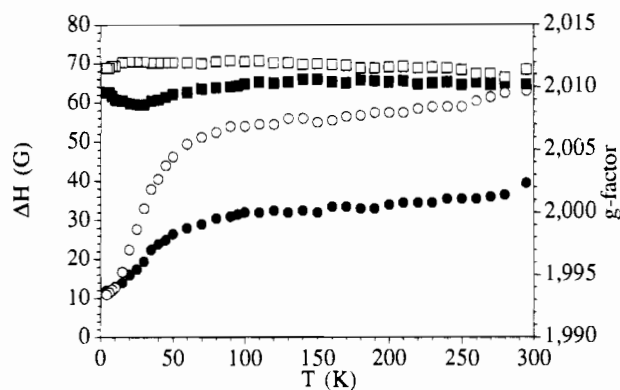
Figure 13. Thermal dependence of the line width (circles) and g factor (squares) for the salts containing diamagnetic anions: α_2-ET$_8$[BW$_{12}$O$_{40}$] (open symbols) and α_1-ET$_8$[SiW$_{12}$O$_{40}$] (full symbols).

factor cannot be fitted to a simple equation as was the behavior in the salts containing diamagnetic anions. This observation suggests that at room temperature the signal of these salts comes from the overlapping of the signal of the ET radicals (conduction electrons) and that of the paramagnetic centers (localized spins). This mixing, partly due to some exchange process, disappears at low temperatures, when the signals of the paramagnetic centers become more intense and for some orientations they are distinct (see Figure 14), as evidenced by rotation diagrams.

The thermal variation of both ESR parameters is displayed in Figure 15. For the three salts ΔH remains almost constant at high temperatures but at lower temperatures ΔH sharply increases. The temperature at which the broadening begins, as well as the amplitude of this broadening, stongly depends on the paramagnetic metal of the polyanion (see Figure 15). Thus, for the Cu^{II} derivative the broadening occurs at temperatures below 160 K, reaching a line width of 327 G at 4.2 K, whereas for the Co^{II} and Fe^{III} salts the broadening begins at lower temperatures (about 70 and 50 K, respectively) and ΔH reaches smaller values at 4.2 K (190 and 126 G, respectively). The g factors also show pronounced thermal dependences. Thus, for the Co^{II} derivative g increases at temperatures below 70 K whereas in the Fe^{III} derivative it decreases at temperatures below 50 K. In the Cu^{II} salt the behavior is more complicated. At temperatures below 160 K the g factor increases to reach a maximum at about 130 K, then it decreases to reach a minimum at about 35 K, and then it increases again (see Figure 15). These behaviors reflect the progressive increase of the line intensity of the metal transition spins.

A line width broadening has already been observed for other organic-inorganic salts with magnetic counterions[6c,d] and attributed to the presence of magnetic interactions between the two magnetic sublattices.[6b] However, in the present case, these broadenings are mainly due to the appearance, at low temperatures, of the ESR signals from the paramagnetic metal centers. In fact, a simple estimation of the intensity ratio between the signal of the radical and that of the metal confirms that at room
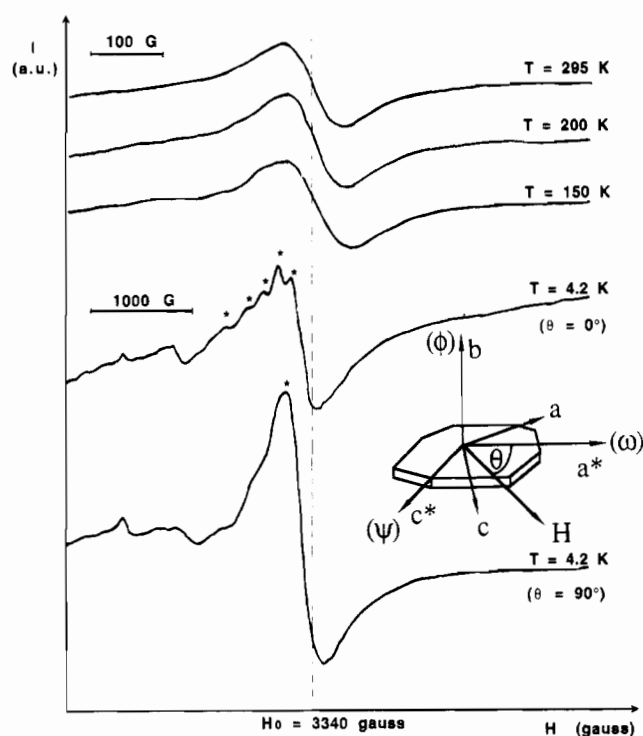
Figure 14. ESR spectra of the salt α_1-ET$_8$[CuW$_{12}$O$_{40}$] at different temperatures. An asterisk denotes the signals coming from the magnetic centers of the polyanions. The inset shows the typical crystal morphology of the title compounds and the crystal orientations used in the ESR rotation experiments.

temperature the signal of the organic radical is about $10-50$ times more intense, depending on the metallic atom, whereas at low temperature this situation is reversed as a consequence of the antiferromagnetic coupling in the organic part. This is also in agreement with the susceptibility data which tends, at low temperature, to the Curie constant value of the constituent metal ion.

Conclusions

The series of radical cation salts presented here demonstrate the possibility of combining inorganic polyoxometalates with organic donors as the BEDT-TTF in order to prepare new hybrid molecular materials in which localized and delocalized magnetic moments coexist. Focusing in the inorganic part, it is to be noticed that the used Keggin polyoxoanions represent the highest charged anions ($4-$, $5-$, and $6-$) used to date in any cation radical salt.[54] Furthermore, we have found that the structures of these salts depend on the size and shape of the polyanion, being independent of the charge.

However, the most interesting informations are coming from the organic sublattice. We are in presence of two related α type crystal structures with two different types of ET stacks in both phases. An inhomogeneous charge distribution between these stacks has been detected from X-ray structural data and
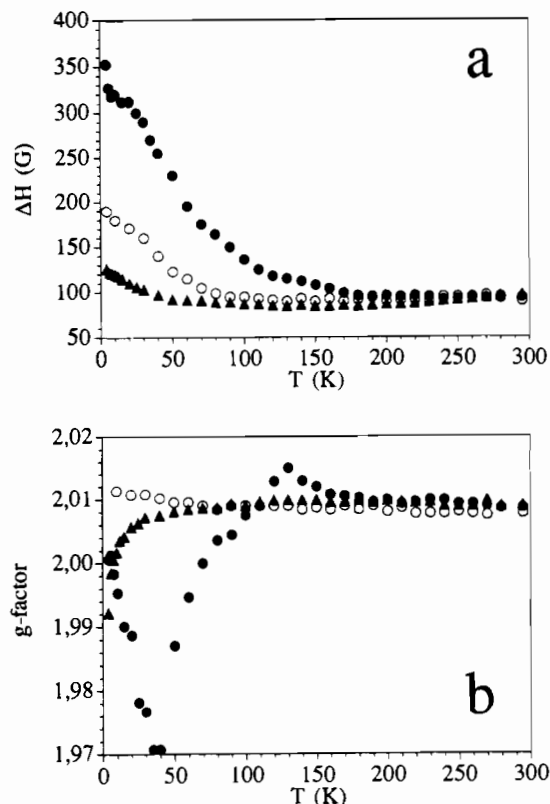
Figure 15. Thermal dependence of the line width (a) and the *g* factor (b) of the salts containing paramagnetic anions: α_1-$ET_8[CoW_{12}O_{40}]$ (open circles), α_1-$ET_8[CuW_{12}O_{40}]$ (full circles), and α_2-$ET_8[FeW_{12}O_{40}]$ (full triangles).

confirmed by the static magnetic measurements. Nevertheless, the clearest evidence comes from both EHT calculations and Raman (and IR) spectra from which local information is obtained. It turns out that the degrees of ionicity are about 0.8 and 0.2 for the molecules of the eclipsed and dimerized stacks, respectively. This situation, which is quite new in these quasi-2-d systems,[55] may be related to the strong electrostatic

interactions produced by the high charges of the polyoxoanion and is inducing an heterogeneous mixed valence state on the organic part. This effect is responsible of the charge localization which occurs progressively at low temperatures and, possibly, accounts for the large Curie component observed in the magnetic behavior.

Finally, the last point deserving attention concerns the magnetic interactions between organic and inorganic blocks. Although in the reported series no magnetic interactions have been detected due to the good isolation of the magnetic ion by the polyoxotungstate framework, one of the main goals in this area is to obtain molecular materials in which localized magnetic moments from the inorganic part are coupled via the conduction electrons of the organic part. The practical synthesis of such materials opens new possibilities as the obtaining of conducting molecular ferromagnets or the stabilization of a superconducting state in a magnetically ordered molecular lattice.[6e] In order to favor this indirect exchange interactions several strategies are now in progress. (i) The first is to increase the organic-inorganic interactions by using substituted Keggin polyanions with one, two or three magnetic centers in the surface of the polyoxoanions, replacing the W atoms. This strategy has already given the first results: Thus, using the monosubstituted polyanions $[XM(H_2O)M'_{11}O_{39}]$ (X = P, Si; M = Mn^{II}, Co^{II}, Ni^{II}, Cr^{III}, Cu^{II}, Fe^{III}, ...; M' = Mo^{VI}, W^{VI}) new ET_8[Keggin] salts have been obtained showing weak, but sizable, ferromagnetic and antiferromagnetic interactions between the metal centers.[25,56] (ii) The second is to increase the magnetic moment in the inorganic part by using magnetic clusters of the type M_4O_{16} (M = Co^{II}, Cu^{II}, Ni^{II}, Mn^{II}, Fe^{II}, Cr^{II}, ...) encapsulated between fragments of Keggin anions. Preliminary results have shown that radical salts of this kind based on ET have been obtained for M = Co^{II} and Mn^{II} but no magnetic interactions between both sublattices can be detected. (iii) The third is to increase the conductivity in the organic sublattice by using ET derivatives with Se substituting S atoms (in the internal or in the external rings). Due to the more extended π orbitals of Se atoms, larger donor-donor contacts should be expected associated with a weaker site localization.

Supporting Information Available: ORTEP drawings showing the atomic labeling and tables giving crystal data and details of the structure determination, atomic coordinates, bond lengths, bond angles, and anisotropic thermal parameters for the four solved structures (25 pages). Ordering information is given on any current masthead page

IC9503601

(54) In the cases where the anionic charge is 5− and 6−, we need to consider the possible presence of protons in the crystal structure (in the form of H_3O^+ or $H_5O_2^+$ groups, as in other related ET radical salts: (a) Mori, H.; Hirabayashi, I.; Tanaka, S.; Maruyama, Y. *Bull. Chem. Soc. Jpn.* **1993**. (b) Shibaeva, R. P.; Korotkov, V. E.; Rosenberg, L. P.; Kushch, N. D.; Laukhina, E. E.; Abashev, G. G.; Yagubskii, E. B.; Buravov, L. I.; Zvarykina, A. V.; Khomenko, A. G. *Synth. Met.* **1991**, *41−43*, 1963. (c) Mori, H.; Hirabayashi, I. *Chem. Lett.* **1987**, 1657. (d) Chasseau, D.; Watkin, D.; Rosseinsky, M.; Kurmoo, M.; Day, P. In *Crystalline Low-Dimensional Organic and Inorganic Solids*, Delhaès, P., Drillon, M., Eds.; Plenum Press: New York, 1987, 317 or attached to the external oxygen atoms of the polyoxoanions, as in the case of other radical salts of Keggin polyoxoanions with TTF: see ref 5c. It is interesting to note that all the salts formed by Keggin anions with charges higher than −4 and big counterions (tetraalkylammonium salts) show the presence of enough protons or small alkaline cations to "reduce" the charge of the Keggin anion to −4: see ref. 7a. The possibility of a reduction of the polyanions has not been contemplated as this would make them even more charged and the solutions in the electrochemical cells would have become dark blue, typical colour of the reduced heteropolyoxoanions (heteropoly blues).

(55) In the α phase of the $(ET)_2I_3$ salt an inhomogeneous redistribution of the charge has been attributed to the transition occurring at 135 K. The final charge distribution shows the simultaneous presence of ET molecules bearing degrees of ionicity of approximately 0.15, 0.5 and 0.9: see ref 36.

(56) Coronado, E.; Galán-Mascarós, J. R.; Gimenez-Saiz, C.; Gómez-García, C. J.; Triki, S.; Delhaès, P. *Mol. Cryst. Liq. Cryst.*, in press.